Записки научных
семинаров ПОМИ
Том 509, 2021 г.

N. M. Bogolyubov, A. G. Pronko

ONE-POINT FUNCTION OF THE FOUR-VERTEX MODEL

Abstract. We consider the four-vertex model on a finite domain of the square lattice with the so-called scalar-product boundary conditions. It can be described in terms of non-intersecting lattice paths which are additionally restricted in their propagation in one of the two spacial directions. We compute the one-point function measuring the probability to obtain a path on a given lattice edge. We also relate this function with another one-point function which can be regarded as a local anti-ferroelectric order parameter.

§1. Introduction

The four-vertex model is a special case of the six-vertex model in which two vertex configurations are frozen out. It was originally introduced in relation with a random tiling model on a cylinder and an infinite strip with free boundary conditions [1, 2]. In the case of finite-size lattices with special choice of fixed boundary conditions it can be related to boxed plane partitions with additional restrictions [3–5].

It is well-known, that the boxed plane partitions exhibit phase separation or "Arctic Circle" phenomena [6]. In more general settings, the same problem can be formulated in terms of the five-vertex model [7]. At its free-fermion point, this model is equivalent to the boxed plane partitions [8]. The four-vertex model can be seen as another special case of the five-vertex model. This case is very interesting, since due to the fixed boundary conditions it corresponds to maximizing the number of vertices typical for an anti-ferroelectric order.

In the present paper, motivated by this observation, we compute the one-point function in the four-vertex model on the finite lattice. Specifically, we consider the boundary conditions such that the partition function

Key words and phrases: vertex models, correlation functions, phase separation phenomena, limit shapes.

This work is supported in part by the Russian Foundation for Basic Research (RFFI), grant No. 19-01-00311. The second author (A.G.P.) acknowledges also support from the BASIS Foundation, grant No. 21-7-1-32-1.

can be given in terms of a scalar product of the off-shell Bethe states. For this reason we call them "scalar product" boundary conditions (in [7] they are referred to as "boxed plane partitions" ones). We consider the homogeneous model and compute the one-point function which corresponds to a local density operator. Equivalently, it can be defined as the probability of obtaining a path on the given edge, in the language of non-intersecting lattice paths. We show that for the four-vertex model this one-point function can be related with another one-point function, which can be used as a local anti-ferroelectric order parameter.

The paper is organized as follows. In Sec. 2 we define the model and compute the partition function. In Sec. 3 we compute the one-point function. In Sec. 4 we apply our results to study the anti-ferroelectric order in the model.

§2. The partition function

We define the four-vertex model as the six-vertex model in which the second and fourth vertices are frozen out, see Fig. 1.

We consider the model on an $M \times 2N$ square lattice with the fixed boundary conditions defined as follows. Using the standard arrow language, we require that all arrows on the external edges are right or up arrows, except on the last N vertical lines at the top boundary and the first N vertical lines of the bottom boundary, where all arrows must be down arrows, see Fig. 2a.

In the equivalent description of local states in terms of solid lines (the edge has the solid line if it contains the left or down arrow, and empty otherwise), the configurations of the four-vertex model are represented in terms of non-intersecting lattice paths with the additional condition that they cannot propagate freely along the horizontal direction (since the fourth type of vertices are forbidden), see Fig. 2b. It can be easily seen that nontrivial configurations exist only if $M \geqslant 2N - 1$.

As usual for a vertex model, the partition function of the four-vertex model is defined as the sum over all possible arrow configurations,

$$Z = \sum_{\mathcal{C}} a^{\nu_a(\mathcal{C})} b^{\nu_b(\mathcal{C})} c^{\nu_c(\mathcal{C})},$$

where $\nu_w(\mathcal{C})$, $w = a, b, c$, denotes the number of vertices with the Boltzmann weight w in the configuration $\mathcal{C}$. A peculiar feature of the four-vertex

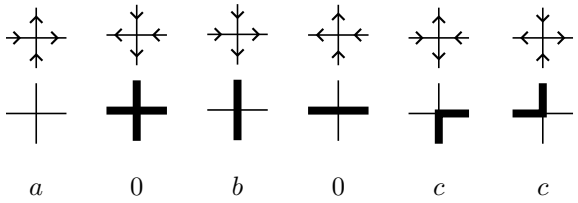

Fig. 1. The six types of vertex configurations in terms of arrows, lines, and their Boltzmann weights in the four-vertex model.

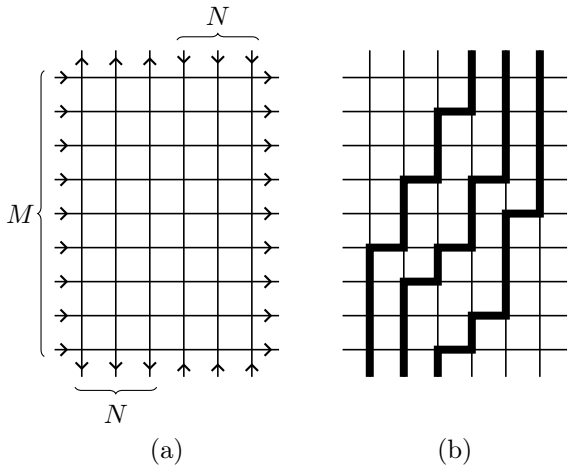

Fig. 2. An $M \times 2N$ lattice with scalar-product boundary conditions.

model with arbitrary fixed boundary conditions (in opposite to open or periodic ones), is that all $\nu_w(\mathcal{C})$ are *independent* of $\mathcal{C}$. This follows from the rather general property of the six-vertex model that if the boundary conditions are fixed, then its first and second, third and fourth, fifth and sixth vertices can appear in configurations only in pairs, see, e.g., a detailed discussion in [9]. Specifically, in our case we have

$$\nu_a = \nu_b = (M-N)N, \qquad \nu_c = 2N^2.$$

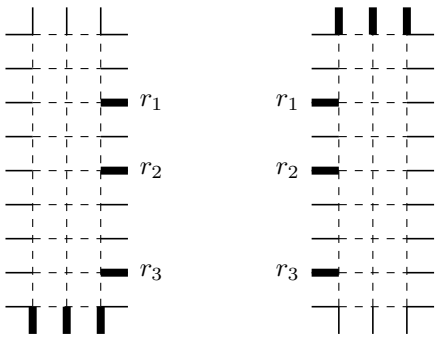

Fig. 3. Graphical interpretation of the functions $\widetilde{\Psi}_3(r_1, r_2, r_3)$ and $\Psi_3(r_1, r_2, r_3)$, respectively. The summation over all admissible path configurations on the dashed edges is assumed.

This means that we can completely ignore values of the Boltzmann weights, e.g., setting them all equal to one, $a = b = c = 1$, and focus on counting path configurations.

To indicate the fact that the partition function depends on geometric parameters of the lattice, we will denote in $Z_{M,N}$. It can be written as a scalar product:

$$Z_{M,N} = \sum_{1 \leqslant r_1 < \ldots < r_N \leqslant M} \widetilde{\Psi}_N(r_1, \ldots, r_N) \Psi_N(r_1, \ldots, r_N).$$

Here, $\widetilde{\Psi}_N(r_1, \ldots, r_N)$ and $\Psi_N(r_1, \ldots, r_N)$ are N-paths "wave functions", and $r_1, \ldots, r_N$ are coordinates of the paths on the right and left boundaries of the left and right $M \times N$ lattices, respectively, see Fig. 3. The two functions are related by

$$\widetilde{\Psi}_N(r_1, \ldots, r_N) = \Psi_N(M - r_N + 1, \ldots, M - r_1 + 1).$$

Note that we count horizontal lines from the top to bottom and that the arguments of the functions are strictly ordered.

More generally, one can write the partition function by dividing the lattice on two unequal portions, having $N - s$ and $N + s$ vertical lines,

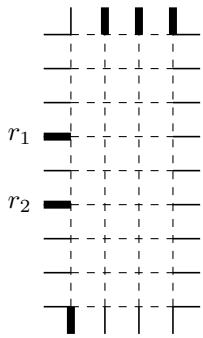

Fig. 4. Graphical interpretation of the function $\Psi_{1,3}(r_1, r_2)$.

respectively. In this way, we have

$$Z_{M,N} = \sum_{1 \leqslant r_1 < \ldots < r_{N-s} \leqslant M} \widetilde{\Psi}_{N-s}(r_1, \ldots, r_{N-s}) \Psi_{s,N}(r_1, \ldots, r_{N-s}), \quad (1)$$

where $\widetilde{\Psi}_{N-s}(r_1, \ldots, r_{N-s})$ is defined as above, and $\Psi_{s,N}(r_1, \ldots, r_{N-s})$ is a generalized 'wave function' corresponding to the $M \times (N+s)$ lattice with N paths exiting at left boundary and s paths exiting at the bottom boundary, see Fig. 4.

We have the following explicit formulas.

Proposition 1. *The 'wave function' of the four-vertex model is given by*

$$\Psi_s(r_1, \ldots, r_s) = \frac{1}{\prod_{k=1}^{s-1} k!} \prod_{1 \leqslant i < j \leqslant s} (r_j - r_i - j + i). \quad (2)$$

Proposition 2. *The modified wave function admits the following representation*

$$\begin{aligned} \Psi_{s,N}(r_1, \ldots, r_{N-s}) = {} & \frac{\prod_{k=1}^{s-1} k!}{\prod_{k=1}^{N} (s+k-1)!} \prod_{i,j=1}^{s} (M - N + 1 + i - j) \\ & \times \prod_{j=1}^{N-s} \prod_{k=1}^{s} (r_j - j - s + k)(M - N + k - r_j + j) \\ & \times \prod_{1 \leqslant i < j \leqslant N-s} (r_j - r_i - j + i). \quad (3) \end{aligned}$$

In order not to interrupt out considerations, we give proofs of these two propositions in appendix A.

It is to be mentioned that these expressions for wave-functions can also be obtained as special homogeneous limits from the Schur functions [10], and, even more generally, in the context of the Quantum Inverse Scattering Method [11], from the off-shell Bethe states [5, 12].

As a simple corollary of Prop. 2, we have the following result for the partition function

$$\begin{aligned} Z_{M,N} = \Psi_{N,N}(\cdot) &= \frac{\prod_{k=1}^{N-1} k!}{\prod_{k=1}^{N}(N+k-1)!} \prod_{i,j=1}^{N} (M-N+1+i-j) \\ &= B(N,N,M+1-2N). \end{aligned} \tag{4}$$

Here, $B(a,b,c)$ denotes the number of boxed plane partition in the $a\times b\times c$ box (see, e.g., [13] and references therein).

§3. The one-point function

Now we turn to calculation of the one-point function. We denote it $G_{M,N}(m,n)$ and define as the probability to obtain a path on the edge located on the mth horizontal line, between the nth and $(n+1)$th vertical lines, see Fig. 5.

Clearly, the path on the given edge is one out of n paths located between the nth and $(n+1)$th vertical lines. Therefore, the one-point function can be given as a sum [12] over $\ell = 1,\dots,n$, where ℓ is the number of the path which appear at the mth horizontal line, among these n paths,

$$G_{M,N}(m,n) = \frac{1}{Z_{M,N}} \sum_{\ell=1}^{n} Z_{M,N;m,n;\ell},$$

where $Z_{M,N;m,n;\ell}$ denote the sum over positions of the remaining $n-1$ paths.

Let us focus on computing $Z_{M,N;m,n;\ell}$. Exploiting the decomposition (1), we have

$$Z_{M,N;m,n;\ell} = \sum_{\substack{1\leqslant r_1<\ldots<r_{\ell-1}<m \\ m<r_{\ell+1}<\ldots<r_n\leqslant M}} \widetilde{\Psi}_n(r_1,\dots,r_n)\Psi_{N-n,N}(r_1,\dots,r_n)\Big|_{r_\ell=m}.$$

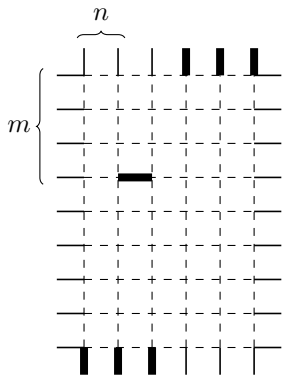

Fig. 5. Definition of the one-point function $G_{M,N}(m,n)$.

Substituting here explicit expressions for the involved functions, see (2) and (3), we get

$$Z_{M,N;m,n;\ell} = \frac{\prod_{k=1}^{N-n-1} k!}{\prod_{k=1}^{N}(k+N-n-1)!\prod_{k=1}^{n-1} k!} \prod_{i,j=1}^{N-n} (M-N+1+i-j)$$
$$\times \sum_{\substack{1\leqslant r_1<\ldots<r_{\ell-1}<m \\ m<r_{\ell+1}<\ldots<r_n\leqslant M}} \prod_{j=1}^{n}\prod_{k=1}^{N-n} (r_j-j-N+n+k)$$
$$\times (M-N+k-r_j+j) \prod_{1\leqslant i<j\leqslant n} (r_j-r_i-j+i)^2 \Big|_{r_\ell=m}. \quad (5)$$

Let us introduce new summation variables p_j, $j=1,\ldots,n-1$, defining them as follows:

$$p_j = \begin{cases} r_j - m - j + \ell, & j = 1,\ldots,\ell-1, \\ r_{j+1} - m - j - 1 + \ell, & j = \ell,\ldots,n-1. \end{cases}$$

An important point need to be taken into account is that the summand in (5) vanishes whenever $r_{j+1} = r_j + 1$. Therefore in terms of the new variables, the sum is performed over the following values:

$$-m+\ell \leqslant p_1 < \ldots < p_{\ell-1} < 0,$$
$$0 < p_\ell < \ldots < p_{n-1} \leqslant M-n-m+\ell.$$

As a result, we arrive at the following expression for the quantity (5):

$$Z_{M,N;m,n;\ell} = \frac{\prod_{k=1}^{N-n-1} k!}{\prod_{k=1}^{N}(N-n+k-1)!\prod_{k=1}^{n-1} k!} \prod_{i,j=1}^{N-n} (M-N+1+i-j)$$

$$\times\, \mu_\ell(0) \sum_{\substack{-m+\ell\leqslant p_1<\ldots<p_{\ell-1}<0 \\ 0<p_\ell<\ldots<p_{n-1}\leqslant M-n-m+\ell}} \prod_{j=1}^{n-1} \mu_\ell(p_j) p_j^2 \prod_{1\leqslant i<j\leqslant n-1} (p_j-p_i)^2. \quad (6)$$

Here $\mu_\ell(p) \equiv \mu_{M,N;m,n;\ell}(p)$ is following function:

$$\mu_\ell(p) = \prod_{k=1}^{N-n} (p+m-\ell-N+n+k)(M-N+k-p-m+\ell). \quad (7)$$

The final step in obtaining a closed expression for the one-point function consists in observation that the sum in (6) is nothing but the sum over minors in an expansion of a determinant of the sum of two matrices, namely

$$\sum_{\substack{p_1<\ldots<p_{\ell-1}\in D_- \\ p_\ell<\ldots<p_{n-1}\in D_+}} \prod_{j=1}^{n-1} f(p_j) \prod_{1\leqslant i<j\leqslant n-1} (p_j-p_i)^2$$

$$= \frac{1}{(\ell-1)!}\partial_z^{\ell-1} \det_{1\leqslant i,j\leqslant n-1} \left[\left(z \sum_{p\in D_-} + \sum_{p\in D_+} \right) f(p) p^{i+j-2} \right] \Bigg|_{z=0}.$$

Here, $f(p)$ is a trial function and $D_\pm$ are two domains of values of the integer variables. This is a rather well-known relation in the random matrix theory, see, e.g. [14].

Summarizing, we formulate our main result concerning the one-point function as follows.

Theorem 1. *The one-point function $G_{M,N}(m,n)$ for the values $m = 1,\ldots,M$ and $n = 1,\ldots,N$, is given by the following expression*

$$G_{M,N}(m,n) = \frac{C_{M,N;n}}{C_{M,N;0}} \sum_{\ell=1}^{n} \frac{\mu_\ell(0)}{(\ell-1)!}$$

$$\times\, \partial_z^{\ell-1} \det_{1\leqslant i,j\leqslant n-1} \left[\left(z \sum_{p=-m+\ell}^{-1} + \sum_{p=1}^{M-n-m+\ell} \right) \mu_\ell(p) p^{i+j} \right] \Bigg|_{z=0}, \quad (8)$$

where

$$C_{M,N;n} = \frac{\prod_{k=1}^{N-n-1} k!}{\prod_{k=1}^{N}(N-n+k-1)! \prod_{k=1}^{n-1} k!} \prod_{i,j=1}^{N-n} (M-N+1+i-j),$$

and the function $\mu_\ell(p) = \mu_{M,N;m,n;\ell}(p)$ *is given by* (7). *The sums defining entries of the determinant in* (8) *are assumed to be equal to zero whenever the final value of the summation variable is less than the starting one.*

Note that the quantity $C_{M,N;0}$ is equal to the partition function $Z_{M,N}$, see (4).

§4. The c-weight vertex probability

To study distribution of the vertices of the fifth and sixth types (see Fig. 1) in the configurations, it is useful to introduce the corresponding correlation function. We will call it c-weight vertex probability and denote $H_{M,N}(m,n)$. We define the function $H_{M,N}(m,n)$ as the probability of having a c-weight vertex at the intersection of mth horizontal and nth vertical lines of the $M \times 2N$ lattice (as usual, we focus on its left-hand size part, $m = 1, \dots, M$ and $n = 1, \dots, N$), analogously to the one-point function $G_{M,N}(m,n)$, see Fig 5.

In the general six-vertex model, the c-weight vertex probability requires calculation of the two-point correlation function which measures states of arrows on two horizontal (or vertical) edges attached to the same vertex. The c-weight vertices are characterized by opposite directions of arrows on these edges. However, in the case of the four-vertex model, since the vertex of the fourth type is excluded (see Fig. 1), it is just sufficient to require that a path must be present on either of the two horizontal edges of the vertex. In other words, for the four-vertex model the following relation is valid:

$$H_{M,N}(m,n) = G_{M,N}(m,n) + G_{M,N}(m,n-1). \tag{9}$$

Here, we assume that $G_{M,N}(m,0) \equiv 0$ by construction.

Using formula (8), one can study the anti-ferroelectric order in the model by making plots of these functions. We give an example of $M = 55$ and $N = 20$ in Fig. 6.

As for the function $G_{M,N}(m,n)$, see Fig. 6a, we find that it has strong oscillating behavior, varying significantly from site to site almost everywhere. It implies that this function is not a proper order parameter for the four-vertex model, contrary to the case of the free-fermion six-vertex

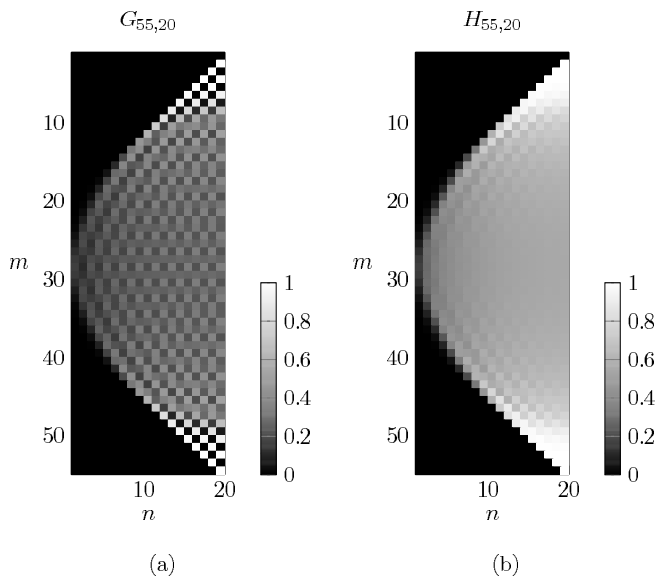

Fig. 6. Density plots of the functions $G_{M,N}(m,n)$ and $H_{M,N}(m,n)$ for $M = 55$, $N = 20$.

model, where the disordered phase dominates in the interior of the domain. In that case the one-point function is smooth almost everywhere [15–19].

As for the function $H_{M,N}(m,n)$, see Fig. 6b, we find that it demonstrates a smooth behavior almost everywhere. This can be easily seen especially when this function is 3D plotted, see Fig. 7. Thus, it is this function that can be used as a proper order parameter to study configurations of the four-vertex model.

Inspecting various cases, we find that the value of $H_{M,N}(m,n)$ in the middle of the lattice ($m \approx M/2$, $n \approx N$) depends on the ratio M/N: it decreases as M increases, and tends to 1 as M approaches the limiting case $M = 2N - 1$, at which there exists just only one configuration, demonstrating the total anti-ferroelectric order.

From the plots it is obvious that the model demonstrates phase separation phenomena: the whole $M \times 2N$ lattice is divided on four regions of the ferroelectric order and one region of the anti-ferroelectric order. As Fig. 6b suggests, the curve separating these regions definitely is neither

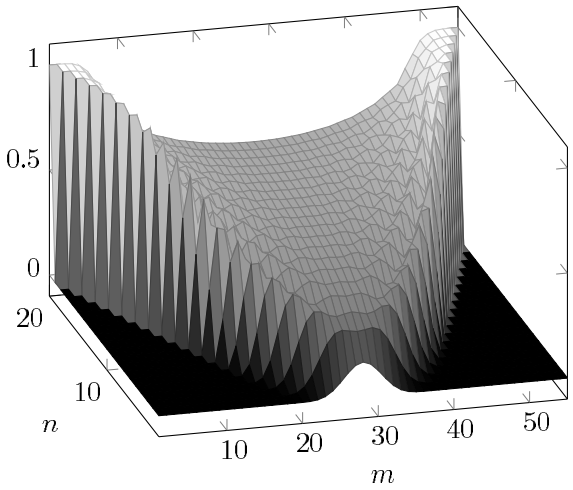

Fig. 7. Plot of the function $H_{M,N}(m,n)$, $M=55$, $N=20$.

an ellipse nor consists of any portions of it. Indeed, in the scaling limit where $M,N\to\infty$ with the ratio M/N kept fixed, this curve must tend, as $M/N\to 2$, to a square.

The plots also shows (see Fig. 7) that the function $H_{M,N}(m,n)$ has a singular behavior near the curve separating phases. Presumably, it has a step-wise behavior in the scaling limit, rather than the square root singularity typical for the phase separation of order and disorder observed in the six-vertex model (see, e.g., [18]). To obtain more detailed and precise information one has to study expressions (8) and (9) in the scaling limit (M,N,m,n are all large, with their ratios kept fixed).

Appendix §A. The wave functions

Here we will outline proofs of Prop. 1 and Prop. 2.

We start with noting that given the function $\Psi_s(r_1,\dots,r_s)$, one can obtain the function $\Psi_{s+1}(r_1,\dots,r_{s+1})$ by means of the relation

$$\sum_{l_1=r_1+1}^{r_2-1}\dots\sum_{l_s=r_s+1}^{r_{s+1}-1}\Psi_s(l_1,\dots,l_s)=\Psi_{s+1}(r_1,\dots,r_{s+1}). \tag{A.1}$$

Graphically this corresponds to adding a column from the left to the $s \times M$ lattice, see Fig. 8. The initial step assumes that $\Psi_1(r_1) \equiv 1$. Hence, $\Psi_2(r_1, r_2) = r_2 - r_1 - 1$. The remaining part is to show that the wave function (2) is reproduced after applying (A.1).

An important property of the wave function $\Psi_s(r_1, \ldots, r_s)$ is that it vanishes whenever $r_{j+1} = r_j + 1$, $j = 1, \ldots, s-1$. This means that if we introduce the variables

$$\tilde{r}_j = r_j + j,$$

then the new variables again form strictly increasing sequences, $0 \leqslant \tilde{r}_1 < \ldots < \tilde{r}_s \leqslant M - s$. Furthermore, we note that in the new variables the wave function reads

$$\Psi_s(r_1, \ldots, r_s) = \frac{1}{\prod_{k=1}^{s-1} k!} \prod_{1 \leqslant i < j \leqslant s} (\tilde{r}_j - \tilde{r}_i).$$

Rewriting it as the Vandermonde determinant and manipulating with the rows, we can bring it, among other ways, in the following form:

$$\Psi_s(r_1, \ldots, r_s) = \det_{1 \leqslant i,j \leqslant s} \left[\binom{\tilde{r}_j + i - 1}{i - 1} \right].$$

Using the well-known relation

$$\sum_{l=0}^{n} \binom{l+i}{i} = \binom{n+i+1}{i+1}, \tag{A.2}$$

we can now perform the sums in (A.1),

$$\sum_{\tilde{l}_1 = \tilde{r}_1 + 1}^{\tilde{r}_2} \cdots \sum_{\tilde{l}_s = \tilde{r}_s + 1}^{\tilde{r}_{s+1}} \det_{1 \leqslant i,j \leqslant s} \left[\binom{\tilde{l}_j + i - 1}{i - 1} \right]$$
$$= \det_{1 \leqslant i,j \leqslant s} \left[\binom{\tilde{r}_{j+1} + i}{i} - \binom{\tilde{r}_j + i}{i} \right] = \det_{1 \leqslant i,j \leqslant s+1} \left[\binom{\tilde{r}_j + i - 1}{i - 1} \right].$$

The last equality produces exactly the function $\Psi_{s+1}(r_1, \ldots, r_{s+1})$, that proves (A.1).

To prove Prop. 2, one has to show that (3) satisfies the relation

$$\sum_{l_1 = 1}^{r_1 - 1} \cdots \sum_{l_{N-s} = r_{N-s-1} + 1}^{M} \Psi_{s,N}(l_1, \ldots, l_{N-s}) = \Psi_{s+1,N}(r_1, \ldots, r_{N-s-1}).$$

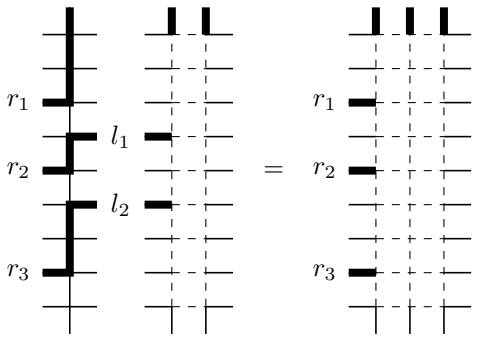

Fig. 8. Graphical interpretation of obtaining the function $\Psi_3(r_1, r_2, r_3)$ from $\Psi_2(l_1, l_2)$; the summation over allowed values of l_1, l_2 is assumed.

Calculations in this case are slightly more involved. We first write the function $\Psi_{s,N}(r_1, \ldots, r_{N-s})$ as a determinant. It is convenient to introduce the following function of N variables:

$$\Phi_N(z_1, \ldots, z_N) = \det_{1 \leqslant i,j \leqslant N} \left[\binom{z_j + i - 1}{s + i - 1} \right]. \tag{A.3}$$

It is fairly easy to see that

$$\Psi_{s,N}(r_1, \ldots, r_{N-s}) = \Phi_N(\tilde{r}_1, \ldots, \tilde{r}_{N-s}, u_1, \ldots, u_s), \tag{A.4}$$

where the variables with tildes are defined as usual, $\tilde{r}_j \equiv r_j + j$, and $u_k \equiv M - N + k$. Next, we perform summations, which in terms of the variables with tildes reads

$$\sum_{\tilde{l}_1 = s}^{\tilde{r}_1 - 1} \sum_{\tilde{l}_2 = \tilde{r}_1 + 1}^{\tilde{r}_2 - 1} \cdots \sum_{\tilde{l}_{N-s} = \tilde{r}_{N-s-1} + 1}^{M-N}.$$

Note that the first sum starts from s (and not 0) and the last sum ends with $M - N$ (and not $M - N + s$) since, as it follows from (A.3) and (A.4), the function $\Psi_{s,N}(r_1, \ldots, r_{N-s})$ vanishes at the values $\tilde{r}_1 = 0, 1, \ldots, s - 1$ and, independently, at $\tilde{r}_{N-s} = M - N + 1, \ldots, M - N + s$. After performing the sums using (A.2), the last step in obtaining the function $\Psi_{s+1,N}(r_1, \ldots, r_{N-s-1})$ can be achieved with the use of the identity

$$\binom{a}{i+1} + \binom{a}{i} = \binom{a+1}{i+1},$$

applied to the last s columns of the determinant, in order to retain the proper polynomial structure of all its N columns.

References

1. W. Li, H. Park, M. Widom, *Finite-size scaling amplitudes in a random tiling model*. — J. Phys. A: Math. Gen. **23** (1990), L573–L580.
2. W. Li, H. Park, *Logarithmic singularity in the surface free energy near commensurate-incommensurate transitions*. — J. Phys. A: Math. Gen. **24** (1991), 257–264.
3. N. M. Bogoliubov, *Four-vertex model and random tilings*. — Theor. Math. Phys. **155** (2008), 523–535.
4. N. M. Bogoliubov, *Four-vertex model*. — J. Math. Sci. (N.Y.) **151** (2008), 2816–2828.
5. N. M. Bogolyubov, C. Malyshev, *Integrable models and combinatorics*. — Russian Math. Surveys **70** (2015), 789–856.
6. H. Cohn, M. Larsen, J. Propp, *The shape of a typical boxed plane partition*. — New York J. Math. **4** (1998), 137–165.
7. J. de Gier, R. Kenyon, S. S. Watson, *Limit shapes for the asymmetric five vertex model*. — Commun. Math. Phys. **385** (2021), 793–836.
8. A. G. Pronko, *The five-vertex model and enumerations of plane partitions*. — J. Math. Sci. (N. Y.) **213** (2016), 756–768.
9. P. Bleher, K. Liechty, *Six-vertex model with partial domain wall boundary conditions: Ferroelectric phase*. — J. Math. Phys. **56** (2015), 023302.
10. I. G. Macdonald, *Symmetric Functions and Hall Polynomials*. — Oxford University Press, Oxford, 2nd edn., 1995.
11. V. E. Korepin, N. M. Bogoliubov, A. G. Izergin, *Quantum Inverse Scattering Method and Correlation Functions*. — Cambridge University Press, Cambridge, 1993.
12. F. Colomo, G. Di Giulio, A. G. Pronko, *Six-vertex model on a finite lattice: integral representations for nonlocal correlation functions*. — Nucl. Phys. B **972** (2021), 115535.
13. D. M. Bressoud, *Proofs and Confirmations: The Story of the Alternating Sign Matrix Conjecture*. — Cambridge University Press, Cambridge, 1999.
14. M. L. Mehta, *Random Matrices*. — Elsevier, Amsterdam, 3rd. ed., 2004.
15. V. E. Korepin, P. Zinn-Justin, *Thermodynamic limit of the six-vertex model with domain wall boundary conditions*. — J. Phys. A **33** (2000), 7053–7066.
16. O. F. Syljuasen, M. B. Zvonarev, *Monte-Carlo simulations of vertex models*. — Phys. Rev. E **70** (2004), 016118.
17. D. Allison, N. Reshetikhin, *Numerical study of the* 6*-vertex model with domain wall boundary conditions*. — Ann. Inst. Fourier (Grenoble) **55** (2005), 1847–1869.

18. V. S. Kapitonov, A. G. Pronko, *Six-vertex model as a Grassmann integral, one-point function, and the arctic ellipse*. — Zap. Nauchn. Semin. POMI **494** (2020), 168–218.
19. P. Belov, N. Reshetikhin, *The two-point correlation function in the six-vertex model*. — arXiv:2012.05182.

St.Petersburg Department
of Steklov Institute of Mathematics, RAS
Fontanka 27, St.Petersburg, Russia
E-mail: bogoliub@pdmi.ras.ru
E-mail: agp@pdmi.ras.ru

Поступило 5 декабря 2021 г.